THE ASTROPHYSICAL JOURNAL, 238:685–698, 1980 June 1

THE LUMINOSITY FUNCTION OF HOT WHITE DWARFS[1]

RICHARD F. GREEN
Hale Observatories,[2] California Institute of Technology
Received 1979 August 20; accepted 1979 December 11

ABSTRACT

An analysis is made of a complete sample of hot white dwarfs, identified spectroscopically from candidates selected for ultraviolet excess without regard to proper motion. A breakdown by spectral type of the entire complete sample of ultraviolet excess objects shows that the hot white dwarfs comprise 64% of the faint blue stars to a mean limiting magnitude of $B = 15.7$. The luminosity function and local space density of hot white dwarfs are derived, giving 1.43 ± 0.28 per 1000 cubic parsecs for $M_v < 12.75$. A model of the local rate of star formation is constructed, which, when combined with white-dwarf cooling theory, satisfactorily reproduces the observed luminosity function. The predicted densities at fainter absolute magnitudes also agree with the observations, although uncertainties in the data do not allow a determination of the change in star formation rate with time. The model predicts a range of scale heights for hot white dwarfs of 220–270 pc, and a total local density of degenerate stars of at least 20 per 1000 cubic parsecs. The assumption of a single population of DA white dwarfs with identical composition is not adequate to explain the observed color-color diagram.

Subject headings: luminosity function — stars: stellar statistics — stars: white dwarfs

I. INTRODUCTION

The luminosity function of white dwarfs contains information valuable for determining the evolution of white dwarfs through cooling processes and the rate of formation of their progenitors on the upper main sequence. Luyten (1958) first produced preliminary estimates of the total space density of white dwarfs from counts of proper-motion objects. Weidemann (1967) made a fundamental synthesis of spectroscopic data from Eggen and Greenstein (1965) and Sandage and Luyten (1967), as well as proper-motion data from Luyten (1963–1966). He derived a luminosity function for comparison with white-dwarf cooling theories of Mestel (1952) and Mestel and Ruderman (1967), using the theory to predict the total local density of white dwarfs. More recently, Sion and Liebert (1977) have made a redetermination from all available spectroscopic and photometric data on white dwarfs. Their comparison with detailed evolutionary models of Lamb and Van Horn (1975) shows generally good agreement to $M_{bol} \approx 14$.

An acknowledged difficulty in these analyses has been isolating a statistically valid sample from heterogeneous observational material. The present paper reports on observations that were made specifically to obtain a complete sample based on ultraviolet excess. Over one-third of the faintest stars were ultimately rejected to create a final complete list of 89 white dwarfs, on which this analysis is based. Only 10 of these were previously classified from proper motion catalogs, indicating that the present survey covers a more substantial volume, especially for the hottest stars.

There are further complications in comparing the observed luminosity function with theoretical cooling curves. One must consider the rate of input of new white dwarfs into the cooling sequence, that is, the rate of formation of their upper-main-sequence progenitors, which may be a changing function of time. The local space density of white dwarfs may also be diluted by dynamical expansion of the white-dwarf disk layer. To study these effects, a model of local star formation is constructed, following Schmidt (1959, 1963). The rate of star formation, the dynamical evolution of mean distances perpendicular to the galactic plane, and the white-dwarf cooling curve from Lamb and Van Horn (1975) are then combined to predict the white-dwarf luminosity function.

The observations and white-dwarf absolute magnitude calibration are discussed in § II, and the observed luminosity function and space density in § III. The construction of the star-formation and dynamical-evolution models is described in § IV. Some remarks on the astrophysical implications of the white-dwarf color-color diagram are found in § V, and a brief summary is presented in § VI.

[1] This paper is a dissertation chapter, published in the form completed in 1977.

[2] Operated jointly by the Carnegie Institution of Washington and the California Institute of Technology.

II. THE OBSERVATIONAL DATA AND ABSOLUTE MAGNITUDE DETERMINATION

The basis for this statistical study is a complete sample of hot white dwarfs selected solely on the basis of ultraviolet excess without regard to proper motion. The objects were chosen from 26 two-color films covering 1434 square degrees above $|b| = 37°$ taken on the Palomar 18 inch (46 cm) Schmidt telescope (Green 1976). Initial visual inspection was later followed by computer processing of most films (Green and Morrill 1978), so the selection process should be relatively free of subjective error. Out of the 20,000 stars on each film brighter than a limit near blue magnitude 16.5, about 10 were isolated for showing the strongest ultraviolet excess. These objects were then observed on the Palomar 1.5 m telescope with the Cassegrain image-tube spectrograph at an inverse dispersion of 280 Å mm^{-1} for classification. The faintest ones were observed by Dr. Maarten Schmidt on the Palomar 5 m telescope with the Cassegrain image-tube spectrograph and, more recently, the SIT spectrograph, at an inverse dispersion of 190 Å mm^{-1}.

Any star with a spectrum containing broad hydrogen Balmer lines or broad helium lines was classified as a white dwarf. Some objects showing no strong spectral features were reobserved photometrically in the Strömgren system, as discussed below, or on the 5 m telescope by Dr. Schmidt or Dr. J. L. Greenstein with the multichannel spectrophotometer, after which classifications were made based on the energy distributions. The difficulty in deciding whether a weak-lined star is degenerate without any knowledge of its kinematics is epitomized in the case of PG 2337 +12 (Green, Greenstein, and Boksenberg 1976), which was originally classified as a white dwarf but turned out to be a cataclysmic variable. Those stars showing the H and K lines of ionized calcium were not included in the sample. The survey was intended to have a color limit of $U - B < -0.4$; it can be seen in the color-color diagrams of Greenstein (1966) and Sandage and Luyten (1969) that a limit of $U - B = -0.5$ cleanly discriminates against the subdwarf G stars and the cooler white dwarfs. The difficulty in distinguishing between the latter two types of objects by either colorimetric or spectroscopic criteria led to the decision to exclude stars with calcium H and K from the final list. Although the importance of extending the luminosity function to cooler degenerates was recognized, the present sample is necessarily incomplete in this $U - B$ color range, and could not have contributed an accurate value.

TABLE 1

BREAKDOWN BY SPECTRAL TYPE

Number	Type
89	White dwarfs
27	Subdwarf B or other hot H absorption spectrum
8	Subdwarf O
4	Quasars
4	Compact or Seyfert galaxies
2	Helium stars
1	Cataclysmic variable
6	Peculiar

A breakdown by spectral type is presented in Table 1. The strongly predominant constituent of the faint blue stars down to the mean limiting magnitude of $B = 15.7$ is seen to be the hot white dwarfs. The table includes the previously known white dwarfs, subdwarfs, quasars, and objects seen to be compact galaxies on the Palomar Sky Survey; the sample was limited to starlike objects, however, and does not include objects obviously extended at the scale of the discovery films, such as blue galaxies or planetary nebulae. Green and Schmidt (1978) discussed the complete sample of quasars. The helium and peculiar stars will be the subject of a future investigation.

The next step in the observational procedure was to measure in the Strömgren four-color system each star classified as a white dwarf. Graham (1972) demonstrated the effectiveness of this color system in yielding direct information on the physical properties of white dwarfs. In particular, the color index $b - y$ is a line-free measure of the continuum in DA stars and was shown to be strongly correlated with the absolute magnitudes derived from trigonometric parallaxes, with a dispersion of only 0.27 mag. Graham found that the index $m_1 = (v - b) - (b - y)$ is a direct determination of the hydrogen line strength, from its correlation with the equivalent width of Hγ. Another major result of his work is the remarkably narrow sequence defined by the DA white dwarfs in the $u - b$, $b - y$ diagram, implying a very low scatter in the value of $\log g$, the surface gravity.

Graham also cautioned that *uvby* is a filter-defined system, so that special care must be taken in the

TABLE 2

STRÖMGREN FILTERS

Band	Central Wavelength (Å)	Full Width at Half-Maximum (Å)	Type
u	3425	370	Schott glass 8 mm UG11 + 1 mm WG3
v	4122	212	Interference
b	4691	217	Interference
y	5500	190	Interference

transformations. The set of filters used in this investigation is described in Table 2; measurement on a scanning spectrometer shows them to be very similar to the filter set described by Crawford and Barnes (1970). To avoid uncertain coincidence corrections for the photometer on the Palomar 1.5 m telescope, standard stars must be chosen fainter than 8th magnitude; consequently, primary-system standards could not be used. In order to take into account specifically the effects of the broadened lines in white dwarfs, a list of secondary standards was compiled from Graham's (1972) *uvby* photometry of white dwarfs, with some redder objects added from his lists of Feige stars (Graham 1970). The average residuals of the transformations were 0.05 mag in V, 0.02 mag in $b - y$, and 0.05 mag in $u - b$, defining the accuracy for a single measurement, with the exception of objects fainter than 16th magnitude, for which systematic errors in centering become important. Since every star was measured in both channels of the dual-channel photometer, each of which was reduced separately, the quoted uncertainty is reduced by a factor of $2^{1/2}$, and many objects were measured on two nights, further increasing the accuracy. Since Strömgren photometry had not been done previously on Palomar, standard mean values of the extinction were not available. The extinction was therefore derived each night in a simultaneous solution for the transformation constants (Huchra 1976). The second-order extinction terms were all assumed to be 0.

The measurement of $b - y$ for each white dwarf in the sample allows the computation of M_V from a linear regression on Graham's (1972) data:

$$M_V = 7.56(b - y) + 11.50\,, \quad \text{with } \sigma = 0.27 \text{ mag.}$$

This determination includes all spectral types; the presence of He I λ4713 absorption in the b-filter does not seem to introduce a significant systematic bias for the DB stars, in face of the larger calibration uncertainties. In cases where multichannel spectrophotometry was available, Greenstein's (1977) monochromatic color indices were also used to derive the absolute magnitude. For stars measured in both systems, the agreement was consistent with Greenstein's quoted uncertainty of 0.6 mag, and the value derived from the Strömgren colors was used for uniformity. Likewise, M_V was determined for those stars with broad-band colors by using the calibration of $B - V$ by Sion and Liebert (1977). Again, comparison of absolute magnitudes obtained from the two calibrations was consistent with the dispersion of their fit of 0.24 mag.

As described above, recent computer processing has expanded the list of candidates found by visual inspection, so that several white dwarfs have been discovered spectroscopically for which photoelectric photometry has not been possible. For two of those DA stars, sufficiently high-quality SIT spectra were obtained that the equivalent width of Hγ could be measured with some accuracy. Graham's (1972) empirical relationship between W(Hγ) (as expressed by m_1) and $b - y$ is very tight, and shows a maximum at W(Hγ) $\sim$ 40 Å. Both the photographic $U - B$ colors and the energy distributions through the slit show that the two objects lie on the blue side of the relation, so that $b - y$ and M_V were estimated for them, with the greater uncertainty noted. The effects of interstellar reddening and absorption were neglected in all cases, because of the relatively small distances of the white dwarfs and their high galactic latitude.

The photoelectric magnitudes were measured in visual light, and the absolute magnitudes were also derived on the V scale. The objects were selected, however, from films that were magnitude-limited in B, so it is necessary to know $B - V$ for the statistical study. It is apparent that $b - y$ would transform directly to $B - V$ if it were not for the presence of strong Hγ, but m_1 is an indicator of the strength of Hγ. A bilinear transformation was therefore derived from the photometry of Graham (1972) and Eggen and Greenstein (1965),

$$B - V = 1.57(b - y) + 0.67m_1 - 0.12\,,$$

with a dispersion of less than 0.02 mag. Types DB and DC were included in this calibration; although there is a small systematic error in the transformation for the DB's, the B magnitudes derived in this way are still much more accurate than photographic magnitudes determined to 0.2 mag.

A summary of the observational data for each object in the sample is found in Table 3, and finding charts for all new discoveries are presented in Figure 4 (Plates 20–22).

III. THE LOCAL SPACE DENSITY AND LUMINOSITY FUNCTION OF WHITE DWARFS

The crucial quantity in the definition of a complete sample for statistical study is the limiting magnitude. The V/V_m method, as discussed by Schmidt (1968), is a powerful test of the completeness of a sample. If V is the volume defined by the observed radial distance to an object and V_m the volume defined by the maximum distance at which the object would still appear in the magnitude-limited sample, then the average of V/V_m would be 0.5, with an uncertainty of $(12n)^{-1/2}$ assuming a uniform distribution for n objects. For a single photograph, the procedure would be to pick a first estimate of the completeness limit near the limiting magnitude of the film and compute $\langle V/V_m \rangle$ from the measured apparent magnitudes. If the value is less than 0.5, the completeness limit is made brighter until $\langle V/V_m \rangle = 0.5$ to within the errors.

The situation is in reality more complicated for two reasons. First, variations in transparency, film sensitivity, and telescope focus produce a different limiting magnitude for each film in the survey. Second, the assumption of uniform space density will not be valid for a population of white dwarfs with a density gradient perpendicular to the plane of the Galaxy.

TABLE 3

COMPLETE SAMPLE OF WHITE DWARFS

R.A. and decl. (1950)	Sp	V	$B-V$	$U-B$	Ref.	V	$b-y$	$u-b$	m_1	Ref.	M_v	$1/V_m'$ (10^{-3} pc^{-3})	Name
$00^h04^m59^s$ +13°19′4	DA	...	...	...		13.02	+0.01	+0.14	+0.04		11.6	0.024	
00 14 21 +09 47.3	DA	15.7	(Bpg)	...		...	...	...	...		11.3	0.021	
00 17 27 +13 36.1	DB	15.22	−0.12	−0.97	(1)	15.24	−0.03	−0.03	+0.09	(2)	11.3	0.015	F4
00 22 52 +08 41.4	DA	15.66	−0.17	−1.01		15.66	−0.11	−0.06	+0.07		10.7	0.0068	
00 37 48 −00 37.6	DA	...	...	...		14.85	+0.05	+0.63	+0.32		11.9	0.049	
00 39 29 +04 53.0	DA	...	...	...		12.89	+0.01	+0.10	+0.05		11.6	0.024	
00 39 37 +10 22.4	DA	...	...	...		15.16	−0.08	−0.18	+0.06		10.9	0.0083	
00 46 02 +07 46.3	DC	...	...	...		15.59	−0.13	−0.44	+0.01		10.5	0.0044	
00 48 33 +00 26.4	DB	...	...	...		15.91	−0.14	−0.34	+0.05		10.4	0.0040	PHL 860
00 48 51 +09 05.1	DA	14.29	+0.08	−0.87		14.29	+0.11	+0.23	+0.02		12.3	0.074	
00 55 51 +01 37.9	DA	14.8	(Bpg)	...		...	...	...	...		*	...	
01 01 13 +04 48.6	DA	14.10	+0.14	−0.50	(1)	14.05	+0.18	+0.53	...		12.9	0.18	G1−45
01 02 05 +09 33.4	DA	...	...	...		14.46	−0.09	−0.03	+0.19		10.8	0.0081	
01 15 21 +15 54.8	DB	13.82	+0.11	−0.80	(3)	13.82	+0.13	+0.27	+0.02	(2)	12.7	0.13	W1516
01 36 15 +15 12.6	DA	...	...	...		14.94	+0.20	+0.55	+0.01		13.0	0.22	
01 42 58 +14 49.7	DA	12.3	(Bpg)	...		...	...	...	...		10.4:	0.0040	
02 32 32 +03 30.6	DA	12.25	−0.25	−1.23	(1)	12.39	−0.07	−0.34	+0.03	(2)	10.4	0.0043	F24
03 02 02 +02 45.7	DA	14.81	−0.25	−1.16	(3)	14.93	−0.17	−0.28	...		10.2	0.0029	F31
09 00 13 +55 26.7	DA	...	...	...		13.84	−0.05	+0.40	+0.49		11.1	0.017	
09 06 30 +59 42.8	DA	...	...	...		15.37	−0.18	−0.41	+0.08		10.1	0.0026	
09 12 27 +53 38.6	DC	13.79	+0.30	−0.66	(4)	13.87	+0.30	+0.62	+0.03	(2)	13.8	*	G195−19
09 33 51 +38 21.0	DA	...	...	...		15.47	−0.09	−0.14	+0.17		10.8	0.0079	
09 35 02 +08 26.8	DA	...	...	...		15.17	+0.14	+0.37	+0.02		12.6	0.11	
09 39 21 +07 11.0	DA	...	...	...		14.90	+0.15	+0.60	+0.18		12.6	0.14	
09 40 16 +06 49.4	DA	13.69	−0.19	−1.03		13.69	−0.10	−0.08	+0.11		10.7	0.0066	
09 48 03 +53 23.4	DO	...	...	...		15.22	(mc: $G-R=-0.80$)				9.8	0.0020	
09 53 10 +02 30.2	DC	...	...	...		15.00	−0.14	−0.46	+0.20		10.4	0.0045	
09 57 16 +03 45.0	DA	...	...	...		15.52	−0.15	−0.28	+0.10		10.4	0.0041	
10 12 23 +00 48.3	DA	...	...	...		14.90	−0.12	−0.30	+0.18		10.6	0.0058	
10 15 23 +07 36.2	DA	...	...	...		15.37	+0.20	+0.57	+0.18		13.0	0.26	
10 22 24 +05 01.5	DA	...	...	...		14.22	0.00	+0.73	+0.32		11.5	0.026	
10 52 54 −08 04.7	DA	...	...	...		15.39	+0.11	+0.69	−0.16		12.3	0.062	
10 55 05 −07 15.3	DA	14.28	+0.32	−0.51	(1)	14.27	+0.23	+0.53	+0.02		13.3	*	L898−25
11 00 34 −14 09.5	DA	...	...	...		15.58	−0.14	−0.31	+0.18		10.4	0.0044	
11 54 32 −07 01.0	DA	...	...	...		14.33	−0.07	+0.04	+0.21		11.0	0.011	
11 56 48 −03 44.6	DA	...	...	...		13.52	+0.04	+0.05	+0.12		11.8	0.035	
12 07 02 −03 16.5	DA	...	...	...		13.53	+0.05	+0.04	+0.12		11.9	0.041	
12 17 23 −06 43.0	DA	...	...	...		15.37	+0.05	+0.09	+0.12		11.9	0.041	
12 32 33 +47 54.2	DA	14.52	+0.06	−0.68	(5)	14.48	−0.05	+0.41	+0.48		11.1	0.015	GD 148
12 34 23 +48 11.9	...	...	...	...		14.38	−0.15	−0.43	+0.21		10.4	0.0045	
12 34 31 +50 31.7	DA	...	...	...		14.73	−0.15	−0.37	+0.16		10.4	0.0043	Ton 90
12 36 44 +47 54.3	...	15.52	−0.27	...		15.52	−0.12	...	...		10.6	0.0053	Ton 96
13 08 41 −09 51.2	DA	15.65	+0.04	−0.84		...	...	...	...		11.5	0.025	
13 09 08 −07 49.3	DA	...	...	...		14.11	+0.07	+0.06	+0.18		12.0	0.052	
14 02 02 +06 33.7	DA	15.61	−0.16	−1.03		15.61	−0.07	−0.08	+0.19		11.0	0.010	
14 03 12 +01 58.6	DA	...	...	...		15.90	−0.16:	+0.03	...		10.3:	0.0035	
14 07 47 +00 33.0	DA	...	...	...		15.66	−0.16	−0.25	+0.16		10.3	0.0037	LB 721

TABLE 3—*Continued*

R.A. and decl. (1950)	Sp	V	$B-V$	$U-B$	Ref.	V	$b-y$	$u-b$	m_1	Ref.	M_v	$1/V_m'$ (10^{-3} pc^{-3})	Name
14 19 49 +06 14.4	DA	...	...	...		16.23	+0.09	+0.66	+0.29		12.2	0.078	
14 21 31 +31 48.5	DA	15.30	−0.12	−1.00	(1)	15.25	−0.14	−0.17	...		10.4	0.0050	Ton 197
14 22 27 +03 33.3	DA	...	...	...		16.46	−0.17	−0.17:	...		10.2	0.0029	
14 25 54 +33 11.1	DA	13.0	(Bpg)	...		...	...	...	...		*	...	
14 27 47 +28 17.0	DA	...	...	...		15.80	−0.07	−0.30	+0.11		11.0	0.010	Ton 203
14 32 57 +29 01.1	DA	...	...	...		16.22	−0.16	−0.27	+0.17		10.2	0.0037	
14 34 29 +28 57.9	DA	...	...	...		15.80	−0.12	−0.23	+0.21		10.6	0.0060	Ton 210
14 46 05 +28 37.6	...	...	...	...		14.54	−0.09	+0.01	+0.27		10.8	0.0086	
14 56 00 +29 49.6	DA	15.61	+0.31	−0.59	(3)	...	...	...	...		13.2	0.34	G166−58
14 59 40 +34 43.7	DA	15.77	−0.07	...		15.77	−0.09	+0.12	+0.29		10.8	0.0088	
15 01 13 +30 04.6	DA	...	...	...			(2 stars in aperture)				...	...	
15 02 03 +35 06.3	DA	15.8	(Bpg)	...		...	...	...	...		*	...	
15 04 09 +29 28.2	DA	15.9	(Bpg)	...		...	...	...	...		*	...	
15 09 25 +32 15.5	DA	14.11	+0.09	−0.65	(5)	14.04	−0.02	+0.42	...		11.3	0.020	GD 178
15 25 18 +42 14.5	DA	...	...	...		16.27	−0.20	−0.21	...		10.0	0.0024	
15 26 19 +44 00.6	DC	15.62	−0.23	−1.16		...	...	...	...		10.6	0.0056	
15 31 35 +44 45.3	DA	...	...	...		15.62	−0.21	−0.17	+0.28		9.9	0.0023	
15 44 42 +48 47.8	DA	...	...	...		12.80	−0.03	−0.27	...		11.3	0.019	
15 47 11 +47 38.6	DA	...	...	...		15.55	−0.09	−0.21	+0.21		10.8	0.0082	
15 49 31 +47 36.4	DB	...	...	...		16.00	(mc: $G-R=-0.72$)				10.5	0.0052	
22 26 29 +09 21.8	DA	...	...	...		14.03	+0.07	+0.12	+0.06		12.0	0.047	
22 26 38 +06 07.4	DA	...	...	...		14.70	−0.03	+0.39	+0.24		11.3	0.018	GD 236
22 35 05 +08 13.2	DA	...	...	...		15.42	−0.13	−0.25	+0.08		10.5	0.0047	
22 44 49 +03 05.9	DC	15.8	(Bpg)	...		...	...	...	...		*	...	
22 46 54 +01 58.7	DA	...	...	...		15.84	−0.09	−0.19	+0.08		10.8	0.0073	
22 54 07 +06 40.8	DA	15.1	(Bpg)	...		...	...	...	...		*	...	
23 03 09 +11 29.3	DA	...	...	...		14.42	−0.03	−0.13	+0.00		11.3	0.015	
23 04 05 +01 19.0	DB	16.02	−0.44	−1.15		16.02	−0.18	−0.59	+0.05		10.1	0.0023	
23 08 45 +05 02.9	DA	15.5	(Bpg)	...		...	...	...	...		*	...	
23 09 50 +10 30.7	DA	13.11	−0.32	−1.23	(3)	13.08	−0.17	−0.36	...		10.2	0.0030	GD 246
23 14 16 +06 24.4	DA	15.6	(Bpg)	...		...	...	...	...		*	...	
23 15 48 +08 55.3	DA	...	...	...		14.49	−0.14	−0.24	+0.08		10.4	0.0041	
23 21 19 +14 14.8	DA	...	...	...		14.66	−0.11	−0.04	+0.10		10.7	0.0063	LB 1181
23 23 27 +12 04.9	DA	14.8	(Bpg)	...		...	...	...	...		*	...	
23 28 12 +10 45.4	DA	...	...	...		15.55	−0.07	+0.13	+0.22		11.0	0.011	LB 1194
23 33 07 −00 14.0	DA	...	...	...		15.99	−0.13	−0.39	+0.10		10.5	0.0047	
23 35 11 +10 39.8	DA	...	...	...		15.55	−0.11	−0.13	+0.15		10.7	0.0066	
23 36 22 +06 19.0	DA	...	...	...		15.60	−0.05	+0.32	+0.33		11.1	0.014	
23 37 32 +07 00.8	DA	...	...	...		13.47	−0.01	+0.07	+0.05		11.4	0.018	
23 49 19 +00 11.6	DA	12.3	(Bpg)	...		...	...	...	...		*	...	
23 53 55 +02 40.5	DA	...	...	...		15.83	−0.13	−0.39	+0.08		10.5	0.0047	
23 58 35 +10 43.8	DA	...	...	...		13.61	−0.07	0.00	+0.08		11.0	0.0098	

REFERENCES.—(1) Eggen and Greenstein 1965; (2) Graham 1972; (3) Eggen 1968; (4) Eggen and Sandage 1967; (5) Eggen and Greenstein 1967.

NOTE.—Only one name is given for previously discovered degenerates. For a complete list of cross references, see McCook and Sion 1977. Objects marked with an asterisk were not included in the determination of the luminosity function, either because no photoelectric photometry was available, or because they lay in a fainter absolute magnitude range in which the sample was clearly incomplete. Those stars with measured $u-b \leq -0.2$ showed very weak absorption, from which a gravity estimate is subject to considerable uncertainty.

The number of white dwarfs on any given film is too small to use the V/V_m test to determine the limit for that film. The initial guess for the completeness limit of each film was made by a visual count of the total number of stars within a 0.54 square degree area in the center of the film. This technique allows a determination of the average number of stars per square degree on the film to an accuracy of better than 10%. The observed surface densities were then compared to those derived by van Rhijn (1929) for the same galactic latitude to get the limiting photographic magnitude accurate to 0.1 mag. Arp's (1965) relationship $B = m_{pg} + 0.1 + 0.1(m_{pg} - 14.0)$ was used to transform to the B system.

Even a complete sample, if selected from a population with a nonuniform space distribution such as a thin-disk system, will produce $\langle V/V_m \rangle < 0.5$. Schmidt (1968) explained that use of the density-weighted volume—in this case, $dV' = dVD(z)$, where $D(z)$ is the normalized density distribution perpendicular to the plane— will return the value of $\langle V'/V_m' \rangle$ to 0.5 for a complete sample.

The V/V_m test was applied to the present sample of white dwarfs by first using the initial estimates of the limiting magnitudes derived from the surface densities. The result was 0.32 ± 0.03, far from completeness. Next, the effect of the nonuniform space distribution was tested by assuming a run of densities of the form $D(z) = \exp(-z/z_0)$, with a scale height of 150 pc. This density weighting increased $\langle V/V_m \rangle$ by only 0.05. The implication is that the sample of white dwarfs initially selected was not complete down to the very limit of each film, and that a space distribution had to be assumed to determine the actual completeness limits from $\langle V'/V_m' \rangle$. Scale heights as a function of absolute magnitude with a range of 245–270 pc were adopted from a detailed model, as discussed in the next section. All the magnitude limits were then made brighter by an equal amount and the test repeated until the sample was considered sufficiently complete for a valid statistical study. With final limiting magnitudes 0.8 mag brighter than those originally determined from the surface densities, over one-third of the faintest stars had been eliminated from the sample to produce $\langle V'/V_m' \rangle = 0.46 \pm 0.03$.

The resulting sample was then used to derive the local luminosity function for hot white dwarfs by means of a method discussed by Schmidt (1975). For each star in a magnitude-limited sample, its contribution to the local space density is $1/V_m'$. Combining the values for all stars in the sample gives a series of weighted delta functions distributed in absolute magnitude, the envelope of which defines the luminosity function. The difficulty again arises that each film has a different completeness limit. The problem can be circumvented by deriving a maximum volume for the entire survey as a function of absolute magnitude. In other words, a white dwarf of given absolute magnitude would define a maximum sampled volume for each field, so its contribution to the luminosity function is 1 divided by the union of all the individual maximum volumes. In the case of overlapped adjacent fields, the area of overlap was assigned to the field with the fainter limiting magnitude, and subtracted from the other. The density weighting was determined by computing z_m from the galactic latitude and magnitude limit for each field, then using the scale height from the model. The derived luminosity function is not sensitive to this choice of scale heights; a factor of 2 change in scale height affects the result by 15%. The contribution of each object to the luminosity function is given in the penultimate column of Table 3.

For presentation purposes, the objects were grouped into half-magnitude bins. The results are presented in Table 4 and Figure 1. The quoted uncertainties are simply statistical, and do not include the effects of

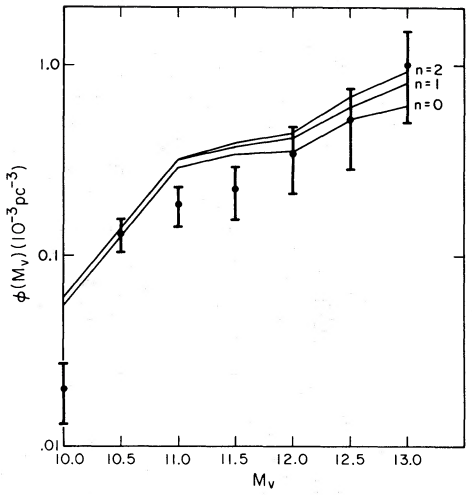

FIG. 1.—White-dwarf luminosity function. For presentation purposes, the data have been grouped into half-magnitude bins. The error bars represent statistical uncertainties only. The smooth curves are model predictions, labeled by the value of the power-law index n.

TABLE 4

LUMINOSITY FUNCTION OF WHITE DWARFS

M_v	10.0	10.5	11.0	11.5	12.0	12.5	13.0
$\phi(M_v)[10^{-3}\ pc^{-3}\ (\frac{1}{2}\ mag)^{-1}]$ ...	0.020 (±0.007)	0.13 (±0.03)	0.19 (±0.04)	0.22 (±0.07)	0.34 (±0.13)	0.52 (±0.23)	0.99 (±0.50)

NOTE.—Errors in parentheses.

errors in photometry or absolute magnitude calibration. The total number of white dwarfs per 1000 cubic parsecs is 1.43 ± 0.28 for $M_V < 12.75$, and with greater uncertainty 2.42 ± 0.57 for $M_V < 13.25$.

The greatest observational uncertainty lies in the two brightest points. At $M_V \lesssim 10.5$, the effective temperature is sufficiently high that the Balmer absorption features become weak. Some possibility for confusion exists in the classification of low-dispersion photographic spectra for these stars, with the error in the sense that some nondegenerates may have been included in the sample for showing weak and slightly broad hydrogen absorption. In addition, there is a calibration problem, in that the linear fit of parallax absolute magnitudes to the $(b - y)$ index compresses a range of 50,000 K into 0.04 mag in $(b - y)$. Since few parallax stars are known at these bright absolute magnitudes, no attempt was made to add a nonlinear correction, but the error is expected to be a systematic tendency to make a small underestimate of the absolute magnitude.

This determination of the luminosity function and space density of hot white dwarfs is the first to be based on a complete sample of spectroscopically identified white dwarfs. Luyten (1958) derived an empirical luminosity function from the fractional contribution of white dwarfs to the general luminosity function of proper-motion stars. Weidemann (1967) constructed luminosity functions from two sets of published data available to him: a large list of objects classified by Luyten (1963–1966) as white dwarfs on the basis of color and proper motion, and the list of spectroscopically identified white dwarfs from Eggen and Greenstein (1965). The inherent difficulties in using those lists are the lack of spectroscopic identifications in the former and the diversity of criteria for selection of the latter. To find limits of relative completeness in apparent magnitude, Weidemann assumed a uniform density distribution of white dwarfs. The V/V_m test applied to the present sample shows that assumption beginning to break down at a mean B magnitude limit of 15.7; Luyten's material reaches to 21st magnitude. Weidemann also did not take into account the area of the sky covered by Eggen and Greenstein's lists. Sion and Liebert (1977) used Weidemann's technique on their larger list of spectroscopically identified white dwarfs, which was subject to the same difficulties. The relative shapes of the luminosity functions so derived appear to be representative. The absolute value of the local space density, however, cannot be accurately determined by this method, as witnessed by the factor of 5 spread in Weidemann's values. For comparison purposes, Weidemann's estimates were transformed to the number density for $M_V < 12.75$, and they bracket the results of the present investigation.

Eggen (1968) has done extensive photoelectric photometry of proper-motion stars, from which he estimated the total number of hot white dwarfs in the first 180 fields of the Lowell Proper Motion Survey (contained in Giclas, Burnham, and Thomas 1971). His defined $U - B$ color limit for this group was approximately the same as that of the present sample. By considering both the completeness limit of his material and the area of coverage, he obtained a lower limit to the mean density of 1 per 1000 cubic parsecs. His use of Luyten's (1965) fractional distribution of hot white dwarfs among proper-motion stars produced a value of 2 per 1000 cubic parsecs. These estimates are in reasonable agreement with the densities derived in this paper.

The luminosity function of white dwarfs contains information about the cooling rate of degenerate stars and about the rate of star formation of the progenitors. The shape of the cooling curve can be compared directly with the luminosity function only if one assumes a constant rate of input of hot white dwarfs; that is, a constant rate of star formation, and that there is no dilution of the space density by a gradual increase in scale height brought about by dynamical interactions. To relax these assumptions, a more detailed model of star formation and dynamical evolution must be computed.

IV. MODELS OF THE RATE OF STAR FORMATION AND WHITE-DWARF LUMINOSITY FUNCTION

To determine the rate of input to the white-dwarf cooling sequence, the rate of star formation of the progenitors must be known as a function of time. The formulation of the problem as developed by Schmidt (1959, 1963) was used in the present investigation. The rate of star formation is derived for the solar neighborhood, assuming it is a smooth function of time for stars of a given mass and that the lifetimes and masses of stars of a given luminosity are not a function of the time of formation; that is, enrichment of composition is neglected. It is observed that the mean distance perpendicular to the plane of the galaxy increases with later spectral type. Since Oort (1958) has shown that the z-distance of galactic clusters increases for later main-sequence turnoff, the further assumption is made that the z-width of a population distribution increases with increasing age. To compensate for this effect, the rates are computed for a cylinder of 1 square parsec cross-sectional area perpendicular to the galactic plane at the Sun.

We shall consider the problem of star formation for the adopted age of the Galaxy as a unit time interval of 1.5×10^{10} years, with $t = 1$ being the present, during which the amount of gas available for star formation was depleted by a factor of 5. Let $N(M_V, t)$ be the number of stars per square parsec formed up to time t in the magnitude interval $M_V - \frac{1}{2}$ to $M_V + \frac{1}{2}$, and $\Psi(M_V)$ be the present rate of formation of stars of brightness M_V, per square parsec. Further, define

$$g(t) = \mathfrak{M}_g(t)/\mathfrak{M}_g(1) \quad (1)$$

as the surface density of gas available for star formation in units of the present density, with $g(1) = 1$,

and $g(0) = 5$. The rate of star formation is then expressed as

$$\frac{dN(M_V, t)}{dt} = \psi(M_V)[g(t)]^n , \quad (2)$$

where the rate is assumed proportional to some power of the gas density. Schmidt's (1963) derivation included a mass-dependent term in the exponent to account for the observed metal abundances in late G-type dwarfs. The white-dwarf luminosity function is very insensitive to the brightest main-sequence stars, so that term was omitted here.

If $\Phi(M_V)$ is defined as the main-sequence luminosity function per square parsec presently observed, and $T(M_V)$ the main-sequence lifetime for stars of absolute magnitude M_V, then from equation (2)

$$\Phi(M_V) = N(M_V, 1) - N[M_V, 1 - T(M_V)]$$
$$= \Psi(M_V) \int_{1-T(M_V)}^{1} [g(t)]^n dt . \quad (3)$$

The main-sequence luminosity function consists of all stars formed less than one main-sequence lifetime ago. For massive stars, $T(M_V) \ll 1.5 \times 10^{10}$ years, and

$$\Phi(M_V) \approx \Psi(M_V) T(M_V) . \quad (4)$$

Schmidt (1959) derived analytical approximations for $g(t)$ by solving for the depletion of the interstellar gas by star formation:

$$n = 1 , \quad g(t) = 5^{1-t} , \quad (5a)$$

$$n = 2 , \quad g(t) = 5/(1 + 4t) . \quad (5b)$$

The above is a brief restatement of the relevant aspects of the problem as formulated by Schmidt. The fundamental data used in the computations are presented in Table 5. The second column lists the masses corresponding to the absolute magnitudes, as given by Schmidt (1963). The third column contains the luminosity function of McCuskey (1966), corrected and smoothed to represent the main sequence. Giant stars contribute significantly to his counts only at absolute magnitudes 0 and +1. The values of the composite luminosity function at these magnitudes were replaced by the corresponding entries of a luminosity function constructed from densities given for main-sequence stars alone. The fourth column lists the values of twice the mean z-distance for the spectral type, as given by Blaauw (1965). The resulting surface density, Φ', follows. One further correction must be applied. McCuskey's luminosity function was derived from counts based on objective prism plates, from which stars were assigned absolute magnitudes based on their spectral types. Evolutionary tracks by Iben (1965, 1966*a*, *b*, *c*, 1967*a*, *b*, 1968) show that stars become brighter and redder as they move away from the zero-age main sequence during core hydrogen burning. Since we are interested in the formation function, $\Psi(M_V)$, the observed luminosity function must be corrected for those evolving stars with spectral types late enough to be assigned the M_V from the next lower bin. The zero-age luminosity function is computed from

$$\Phi(M_V) = \frac{\Phi'(M_V) - c\Phi(M_V - 1)}{(1 - c)} , \quad (6)$$

where c was determined to be 0.36 for masses down to 1.25 $\mathfrak{M}_\odot$. At that point, the evolutionary tracks tend toward the vertical with negligible color change. For 1.25 $\mathfrak{M}_\odot$, $c = 0.13$, and for 1 $\mathfrak{M}_\odot$, $c = 0$. Column (6) shows the corrected luminosity function, and the main-sequence lifetimes from Iben (1965, 1966*a*, *b*, *c*, 1967*a*, *b*, 1968) are presented in the last column.

The derived present rate of star formation per square parsec is given in Table 6 and shown graphically in Figure 2. The main-sequence lifetimes are sufficiently short for $M_V \leq +2$ that equation (4) was used to compute $\Psi(M_V)$, while the values for fainter magnitudes depend on the choice of models. This combination of data yields a function which, at the bright end, is 3 times larger than that derived by Schmidt (1963). The primary reason is that the factor of 2.5 correction for the contribution of giants to the luminosity function of van Rhijn (1936) is not applicable to

TABLE 5

FUNDAMENTAL DATA

M_v (1)	$\mathfrak{M}/\mathfrak{M}_\odot$ (2)	ϕ_{MS} (10^{-4} pc^{-3}) (3)	$2\langle\|z\|\rangle$ (pc) (4)	Φ' (pc^{-2}) (5)	Φ (pc^{-2}) (6)	T (1.5×10^{10} yr) (7)
−4	26	0.0040	100	0.000040	0.000063	0.0006
−3	15	0.013	100	0.00013	0.00017	0.0008
−2	9	0.063	100	0.00063	0.00089	0.0021
−1	6	0.24	100	0.0024	0.0032	0.0043
0	4	0.87	120	0.010	0.014	0.011
+1	2.8	2.4	140	0.034	0.045	0.025
+2	2.2	5.8	170	0.10	0.13	0.051
+3	1.6	12	260	0.31	0.41	0.13
+4	1.3	18	360	0.65	0.58	0.27
+5	1.0	36	540	1.9	1.8	0.67
+6	...	46	540	2.5	2.5	...

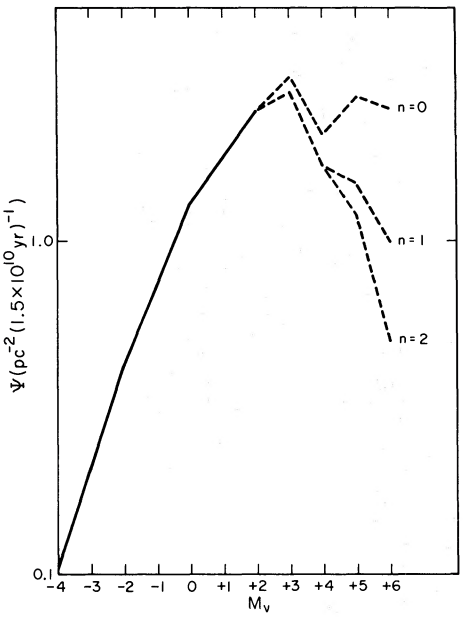

FIG. 2.—Present rate of star formation

that of McCuskey (1966), even though the two functions are nearly identical. Ostriker, Richstone, and Thuan (1974) performed a similar exercise, but obtained an even steeper star formation rate with magnitude, because they claimed that only 12% of the brightest stars are on the main sequence. This value was derived from the luminosity function of Upgren (1963), but his counts were incomplete in that absolute magnitude range, so their value of 12% is probably not correct.

The white-dwarf luminosity function is determined by the rate of star formation for spectral types G and earlier, and by the white-dwarf cooling curve. Recent models have been computed by Lamb and Van Horn (1975) with improved equations of state and explicit treatment of white-dwarf crystallization and envelope convection. For $10.0 < M_V < 13.5$, the cooling time from their models may still be adequately approximated by $t_c \propto L/L_\odot{}^{-5/7}$, or $\log t_c \propto (2/7)M_{\rm bol}$ (Mestel 1952). Their models for a 1 $\mathfrak{M}_\odot$ pure carbon core were used to set the cooling time scale. New bolometric corrections from Greenstein (1977) allowed conversion to M_V. The relationship is a quadratic, which was approximated by two straight lines:

$$M_V = 0.34M_{\rm bol} + 7.7\,,$$
$$\log t_c = 0.84M_V - 11.19, \quad M_V < 11.3\,;$$
$$M_V = 0.89M_{\rm bol} + 1.9\,,$$
$$\log t_c = 0.32M_V - 5.33, \quad M_V > 11.3\,. \qquad (7)$$

The cooling time expressions scale the result to a mass of 0.7 $\mathfrak{M}_\odot$ and are expressed in units of 1.5×10^{10} years. The modeling process assumes that all stars leaving the main sequence evolve into identical hot white dwarfs that follow this cooling curve. This assumption will be examined further in § V.

Values for the thickness of the white-dwarf disk are necessary to convert the predicted surface densities back into volume densities for comparison with the observations. The equivalent width of the disk for a given type of main-sequence star was assumed to be twice the mean z-distance, which increases toward fainter absolute magnitudes, as shown in Table 3. It is further assumed that this increase is correlated with the greater mean age of the fainter stars and reflects a mean z-velocity that grows with time. Stars may add energy to their orbits through several mechanisms, such as binary encounters with massive interstellar clouds as proposed by Spitzer and Schwarzschild (1953), passage through spiral arms, or experiencing other large-scale fluctuations in the gravitational potential. For purposes of this investigation, the increase in mean z-distance will be described by an empirical relation fit to the data. Using the lifetimes in Table 3, we obtain

$$2\langle|z|\rangle = 100 + 700t^{0.789}\ \text{pc}\,, \qquad (8)$$

which is held at a constant value of 540 pc once that maximum is reached. The form of this relation suggests that the average z-distance for stars of the same age be expressed as a constant plus an exponential growth with time. For a given absolute magnitude, the observed mean z-distance is the average over stars of all ages

$$\langle|z(M_V)|\rangle = \frac{\int_0^{T(M_V)} (z_0 + at^p)\{g[t+1-T(M_V)]\}^n dt}{\int_0^{T(M_V)} \{g[t+1-T(M_V)]\}^n dt}\,. \qquad (9)$$

For $n = 0$ the solution is straightforward:

$$\langle|z(M_V)|\rangle = z_0 + \frac{a[T(M_V)]^p}{p+1}\,, \qquad (10)$$

TABLE 6

PRESENT STAR-FORMATION RATE

M_v	−4	−3	−2	−1	0	+1	+2	+3	+4	+5	+6	Model
$\Psi(pc^{-2}/1.5\times10^{10}\,yr)$..	0.11	0.21	0.42	0.74	1.3	1.8	2.5	3.1	2.1	2.7	2.5	$n=0$
								2.8	1.7	1.5	1.0	$n=1$
								2.8	1.7	1.2	0.5	$n=2$

which transforms equation (8) to give the growth in mean z-distance with time for any single-age population:

$$2\langle|z|\rangle = 100 + 1250t^{0.789}\ \text{pc}\,. \tag{11}$$

For the other models, the exact solutions are

$$\langle|z|\rangle = z_0 + aT^{p+1}\frac{\ln 5}{(1-5^{-T})} \times \Gamma(p+1)\gamma^*(p+1, T\ln 5), \quad n=1\,, \tag{12}$$

where γ^* is the incomplete gamma function, and

$$\langle|z|\rangle = z_0 + \frac{aT^p}{(p+1)}\frac{5}{(5-4T)} \times {}_2F_1\left[2, p+1; p+2; \frac{-4T}{(5-4T)}\right], \quad n=2\,, \tag{13}$$

where ${}_2F_1$ is the Gaussian confluent hypergeometric function. Happily, power series expansions of equations (12) and (13) produce leading terms identical to that of equation (10) and first-order terms that make less than 15% difference for the largest value of T, with higher-order terms of alternating sign. Since the analytic g's were approximations in the first place, equation (11) was used to describe the time evolution of mean z-distances for all the models.

For a given white-dwarf absolute magnitude, the mean z-distance is the average of the evolved values for all white-dwarf progenitors:

$$\langle|z|\rangle = \frac{\sum \Psi(M_V)\{g[1-t(\text{WD})]\}^n\{z_0 + a[t(\text{WD})]^p\}}{\sum \Psi(M_V)\{g[1-t(\text{WD})]\}^n}\,. \tag{14}$$

The time spent by the stars in the red-giant phase has been neglected, with the age of the white dwarf given by $T(M_V) + t_c(\text{WD})$.

The differential luminosity function itself is calculated by considering the formation of progenitors during the cooling interval defined by the half-magnitude bins

$$\Phi[M_V(\text{WD})] = \sum \Psi(M_V) \times \int_{1-T(M_V)-t_c[M_V(\text{WD})+1/4]}^{1-T(M_V)-t_c[M_V(\text{WD})-1/4]} [g(t)]^n dt\,. \tag{15}$$

The sum was truncated above 6 $\mathfrak{M}_\odot$, but the higher masses make a negligible contribution and the results are insensitive to this cutoff.

The models derived are presented in Table 7 and shown in Figure 1 superposed on the data. In regard to Figure 1, it is important to remember that no vertical scaling is possible; the model is a prediction independent of the white dwarf data. The fit is seen to be satisfactory. A formal determination of the "goodness of fit" gives preference to the $n = 0$ case, although all are acceptable. The absolute level is directly affected by the computed disk thickness, but the limits of the range of mean z-distances allowed by the uncertainties in the data can be no less than a factor of 2. The detailed predictions about the white-dwarf disk therefore have not been strongly tested, although an extremely thin or a halo distribution for the stars in the sample has probably been ruled out. The model is seen to deviate significantly from the data at the bright end. Two factors are contributing. The theoretical cooling curve is very steep for the hottest objects, so that fewer bright white dwarfs may be expected than the $L^{-5/7}$ relation predicts. As discussed above, the absolute magnitude calibration also becomes very insensitive at the hot end, with a 50,000 K temperature range compressed into 0.04 mag in $b-y$. Small uncertainties in the photometry produce large errors in the absolute

TABLE 7

MODEL LUMINOSITY FUNCTIONS

		$n=0$			$n=1$			$n=2$		
M_v	t_c (1.5×10^{10} yr)	$2\langle\|z\|\rangle$ (pc)	Φ (pc^{-2})	ϕ ($10^{-3}\,\text{pc}^{-3}$)	$2\langle\|z\|\rangle$ (pc)	Φ (pc^{-2})	ϕ ($10^{-3}\,\text{pc}^{-3}$)	$2\langle\|z\|\rangle$ (pc)	Φ (pc^{-2})	ϕ ($10^{-3}\,\text{pc}^{-3}$)
9.75	0.0010	426	0.024	0.055	482	0.029	0.060	517	0.031	0.059
10.25	0.0027	432	0.057	0.13	489	0.069	0.14	524	0.074	0.14
10.75	0.0067	438	0.13	0.29	496	0.16	0.32	531	0.18	0.33
11.25	0.016	453	0.16	0.34	510	0.19	0.37	540	0.21	0.39
11.75	0.027	470	0.17	0.35	526	0.22	0.41	540	0.24	0.44
12.25	0.039	488	0.26	0.51	540	0.33	0.61	540	0.37	0.69
12.75	0.057	514	0.33	0.62	540	0.44	0.81	540	0.50	0.93
13.25	0.080	540			540					

magnitude determination, and the probable departure from linearity of the calibration leads to a systematic underestimation of the luminosity when using the linear fit. No correction to the luminosity function has been attempted, but the $M_V = 10.0$ points would be pulled up closer to the model curves.

The model z-distribution can be tested directly by the prediction of counts of hot white dwarfs at fainter apparent magnitudes. With the technique of constructing an $m - \log \pi$ table, the number per square degree of the sky can be computed for any limiting magnitude, given the observed luminosity function and model scale heights. Since the density distributions of main-sequence stars can be adequately approximated by $D(z) = \exp(-z/z_0)$, this form was assumed to characterize the white-dwarf distribution as well, with the consequence that $z_0 = \langle |z(M_V)| \rangle$, as given in Table 5. The difficulty in using this technique of $m - \log \pi$ is that the observed counts must be sufficiently accurate and include a large enough volume to select a meaningfully small range of scale heights from the predictions. The z-distances under consideration must therefore be great enough to indicate densities substantially lower than the local value. The local densities in the luminosity function are not fixed, however, because they were determined for the present sample from volume elements weighted by exponentials with the same scale heights. The net result is a reduction in the sensitivity of the predicted surface densities to changes in z_0, requiring even larger values of z for a significant test.

Sandage and Luyten (1967) give a preliminary list of spectroscopic classifications of a sample chosen for ultraviolet excess. A re-examination of that material produces a sample, with color properties similar to the sample in this investigation, that contains 24 objects, or 0.6 white dwarfs per square degree to a limiting magnitude of 17.75. Because of the similarity in selection by color, the sample was assumed to include all white dwarfs with $M_V < 13.25$; this assumption is not critical since an error in the estimated color limit leading to the exclusion of the last half-magnitude of the luminosity function would reduce the result by only 10%. The predicted counts are 0.6 per square degree and are insensitive to the small changes of scale height between the models, with even a factor of 2 decrease in scale height yielding the same result. Although the agreement gives confidence in the present luminosity function, the counts to 18th magnitude do not include sufficient volume to test the model density distribution, and a fainter limit must be sought.

The counts at 20th magnitude can also be predicted, to be compared with work in progress on a plate with that magnitude limit by Schmidt and Ulfbeck (1977). Spectra of 37 ultraviolet-excess objects form the basis for a rough preliminary guess of 1–2.5 hot white dwarfs per square degree on that plate. To 19.75 mag, the model scale heights lead to a prediction of 3.4 per square degree for $M_V < 12.75$. The as yet uncertain color and magnitude limits make the comparison difficult. The predicted counts go down to 1.6 per square degree if the scale height is made one-half the assumed value. Hence, reliable surface densities of hot white dwarfs at 20th magnitude or fainter will be a powerful test for the density distribution.

A decision about the correct choice of power-law indices, n, in the model may be aided by an estimate of the luminosity function for white dwarfs of fainter absolute magnitudes. Weidemann (1967) noted that the distribution of known white dwarfs was consistent with uniformity out to a distance of approximately 6 pc from the Sun. For the present estimate, we will use five white dwarfs with $M_V > 13.25$ known within 6.2 pc: van Maanen's star, G175 – 34B, L97 – 12, LP 658 – 2, and G240 – 72. The resulting space density is 5 per 1000 cubic parsecs for $M_V < 15.7$. The objects were discovered because of their high proper motions; all are greater than $1''.5\ \mathrm{yr}^{-1}$. The corresponding tangential velocities range from 49 to 68 km s^{-1}. On the assumption that the progenitors of these objects were the Population I main sequence stars used in constructing the star formation model, this sample of white dwarfs represents only the high-velocity fraction of the total population in this absolute magnitude range. A rough estimate for a correction may be obtained by considering the fraction of stars with speeds above a specified cutoff in a Maxwellian distribution. This approximation neglects the asymmetry from the solar motion, which produces a larger high-velocity tail in the real distribution of tangential speeds. The choice of a value of the cutoff in speed lower than that indicated by the data should help compensate for this underestimate. The computed fraction depends only on the ratio of the cutoff speed to the rms single component of velocity, with the range of this parameter chosen around 1.5. The result suggests that as few as 50% of the total number of white dwarfs within 6.2 pc of the Sun with $13.25 < M_V < 15.7$ have been discovered to date. The corrected space density for these objects becomes 10 ± 5 per 1000 cubic parsecs. The star-formation model predicts 11, 18, and 30 per 1000 cubic parsecs for $n = 0$, 1, and 2, respectively. Although preference is given to the $n = 0$ model, the difficulties in estimating the large correction preclude the selection of a single value for n. For that value to be determined by white dwarfs alone, an accurate density of the cool degenerates will be required.

As an aside, it is interesting to note that three of the 10 nearest white dwarfs of all absolute magnitudes are faint members of multiple systems and would not be detectable in an ultraviolet excess survey, especially at 10 times the distance. This multiplicity factor might explain why the model predictions for the total density in hot white dwarfs exceed the observed value by 30–40%.

The model can be used to derive the total local density in white dwarfs. To do that, the total number of upper-main-sequence stars formed between times 0 and $1 - T(M_V) - t_c(13.25)$ is computed. The predicted total densities are given in Table 8, assuming a mean z-distance for cool degenerates of 270 pc and that all

TABLE 8

PREDICTED TOTAL DENSITY IN WHITE DWARFS

Model n	Number Density (10^{-3} pc^{-3})	Volume Density ($\mathfrak{M}_\odot\ 10^{-3}$ pc^{-3})	Surface Density ($\mathfrak{M}_\odot$ pc^{-2})
0	21	15	8
1	50	35	19
2	104	73	39

white dwarfs may be characterized by a mean mass of $0.7\ \mathfrak{M}_\odot$. From the minimum value of $n = 0$, degenerate stars account for at least 10% of the mass density in the solar neighborhood (Oort 1965) and represent at least 22% of the number of stars presently on the main sequence (McCuskey 1966). The available data leave open the possibility that the entire unknown mass component of the total local density may be accounted for by degenerate stars.

V. THE WHITE-DWARF COLOR-COLOR DIAGRAM

Further direct information about the physical properties of white dwarfs may be obtained from the color-color diagram. Figure 3 plots the Strömgren indices $u - b$ versus $b - y$ for all stars measured accurately in the course of the observational program, including those fainter objects later dropped from the complete sample. The two indices measure the Balmer jump and Paschen continuum, respectively, for DA stars. A sample of hydrogen white dwarfs of identical composition and surface gravity would therefore define a cooling locus in this plane.

Synthesized colors from model atmospheres by Wickramasinghe and Strittmatter (1972) and by Wehrse (1975) have been superposed on the data. The accuracy of the fit to any given curve can be estimated from the cross, representing the mean measuring uncertainties of 0.015 mag in $b - y$ and 0.035 mag in $u - b$. The cooler stars seem to be well fitted by the log $g = 8$ models, as found by Weidemann (1975) and Wehrse (1975), but the hot stars show considerable scatter. For the stars between 15,000 and 25,000 K, most of the scatter can probably be explained if the objects near the blackbody line and the helium model loci are in fact spectral type DB. The classification spectra were often not of sufficiently high quality to identify weak He absorption features, which would be nearly absent near the blackbody line. A determination of the distribution of white-dwarf spectral types can therefore not be made from this sample, and must be obtained from the work of Sion and Liebert (1977) or Greenstein (1977).

More puzzling is the large scatter of the hottest white dwarfs. Some fraction of the objects are undoubtedly composite, with a redder $b - y$ than the Balmer jump would indicate, and some may be hot subdwarfs of lower surface gravity. The formal dispersion for the objects hotter than 25,000 K around even the best fitted line is twice the measuring uncertainty. Within that uncertainty, they span all the loci between the upper main sequence and the blackbody line. One explanation could be a larger dispersion in log g than previously determined, but Graham's (1972) sample should then have shown more scatter for the cool degenerates. When H^- becomes the dominant source of opacity, the magnitude of the Balmer jump becomes very sensitive to the value of log g, and the tightness of Graham's data suggests a small dispersion in the surface gravity.

Another more cogent explanation involves compositional variations in the cores and remnant atmospheres of the white-dwarf progenitors after the red-giant phase. If the premise of Van Horn (1968) and Lamb and Van Horn (1975) is correct, then the phase transition to the solid state adds the latent heat of crystallization to the internal energy and slows the cooling rate. Depending on the internal compositions

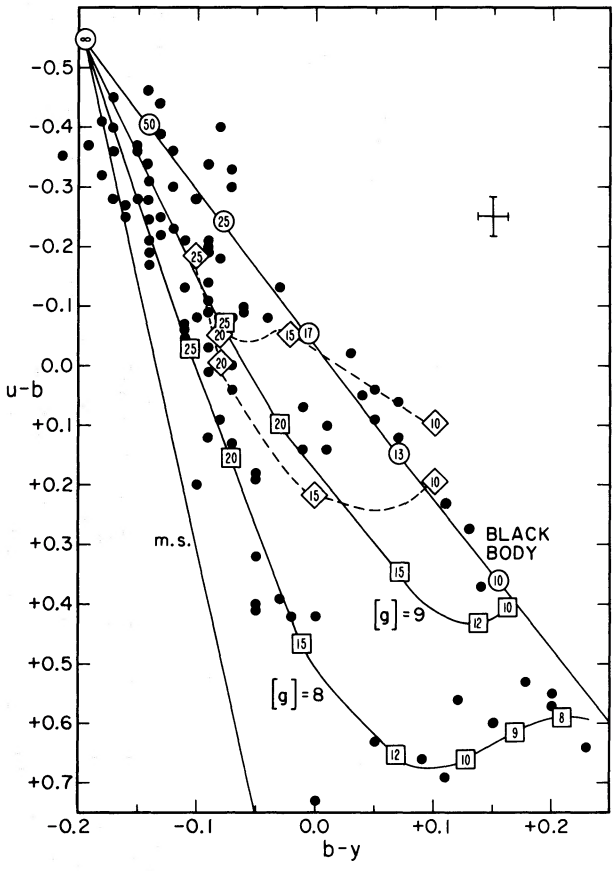

FIG. 3.—White-dwarf Strömgren color-color diagram. Superposed on the data are model loci, with temperatures given in units of 1000 K. The observational main sequence is from Slettebak, Wright, and Graham (1968), and the blackbody line is from Matsushima (1969). The solid lines connect DA models with log $g = 8$ and 9 from Wickramasinghe and Strittmatter (1972), while the dashed lines mark hydrogen-deficient models from the same paper. The coolest three points on the log $g = 8$ curve are due to Wehrse (1975). The cross represents the uncertainty in measurement; note the large scatter in the hottest objects.

of the white dwarfs, several crystallization sequences could be formed. Tapia's (1977) observations seems to support this hypothesis, in that they show two distinct sequences of luminosity versus effective temperature, based on models fitted to the color indices devised by Wickramasinghe and Strittmatter (1972).[3] The broad-band measurements of Eggen and Greenstein (1965), the Strömgren values of Graham (1972), and the monochromatic magnitudes of Greenstein (1977), when plotted as a Balmer-jump index versus absolute magnitude, show evidence for more than one cooling sequence. It must be remembered at the same time that the absolute magnitude forms a single sequence with $b - y$, a measure of temperature for DA stars from the Paschen continuum alone. With the Balmer-jump temperature index finding more than one sequence, the possibility must be considered of a range of compositions in DA atmospheres. A variation in the hydrogen-to-helium ratio from pure hydrogen to that of the extreme DB's might not be unexpected if the evolutionary histories of the progenitors include varying degrees of convective mixing or gravitational diffusion.

The observational evidence makes clear that hot white dwarfs do not fall along a single theoretical cooling sequence. Unfortunately, the spectra of these weak and broad-lined objects do not contain much information about their composition. Perhaps a future look at some of the ultraviolet resonance lines from space will help us begin to understand this enigma.

VI. SUMMARY

The major results of this investigation may be summarized as follows:

The local luminosity function of hot white dwarfs is presented in Figure 1 and Table 2. The total local density of white dwarfs is 1.43 ± 0.28 per 1000 cubic parsecs for $M_V < 12.75$.

[3] Weidemann (1978), however, argues strongly against this hypothesis.

A model of the local rate of star formation and of disk-layer expansion, when combined with white-dwarf cooling theory, adequately reproduces the observed luminosity function as shown in Figure 1. The extension to fainter absolute magnitudes also agrees with observations, although the uncertainties in the data preclude a determination of the change in star-formation rate. The model predicts a range of scale heights for hot white dwarfs of 220–270 pc, which will be tested by the observed surface density at 20th magnitude. The total local density in degenerate stars expected from the models is at least 20 per 1000 cubic parsecs.

The assumption of a single population of hydrogen white dwarfs with identical composition is not adequate to explain the scatter in the Strömgren $u - b$, $b - y$ diagram.

The most important conclusion, however, is that the theoretical understanding of both main-sequence lifetimes and the hot end of the white-dwarf cooling curve gives satisfactory agreement with the observational data.

I gratefully acknowledge the advice, participation, and support of Dr. Maarten Schmidt; the instruction on faint blue stars by Dr. Jesse Greenstein; Dr. Allan Sandage for providing encouragement and data prior to publication; the late Messrs. Dennis Palm and Eugene Hancock, and Mr. Chip Williams, who have assisted at the telescopes with skill and friendship; the ongoing help with electronics from Messrs. Martin Olsiewski, Bud Smith, Larry Blakée, and Bob Cadman; the valued collaboration in film scanning of Mr. Michael Morrill at JPL; the constant help in preparation of the manuscript by Mrs. Helen Holloway; and the continuing assistance and encouragement in this project by Mrs. Joan Auerbach Green.

This research was supported in part by the National Science Foundation under grant AST75-22923 A02.

REFERENCES

Arp, H. C. 1965, in *Stars and Stellar Systems*, Vol. **5** (Chicago: University of Chicago Press), p. 455.
Blaauw, A. 1965, in *Stars and Stellar Systems*, Vol. **5** (Chicago: University of Chicago Press), p. 435.
Crawford, D. L., and Barnes, J. V. 1970, *A.J.*, **75**, 978.
Eggen, O. J. 1968, *Ap. J. Suppl.*, **16**, 97.
Eggen, O. J., and Greenstein, J. L. 1965, *Ap. J.*, **141**, 83.
———. 1967, *Ap. J.*, **150**, 927.
Eggen, O. J., and Sandage, A. 1967, *Ap. J.*, **148**, 911.
Giclas, H. L., Burnham, R., Jr., and Thomas, N. G. 1971, *Lowell Proper Motion Survey* (Flagstaff, Ariz.: Lowell Observatory).
Graham, J. A. 1970, *Pub. A.S.P.*, **82**, 1305.
———. 1972, *A.J.*, **77**, 144.
Green, R. 1976, *Pub. A.S.P.*, **88**, 665.
Green, R., Greenstein, J. L., and Boksenberg, A. 1976, *Pub. A.S.P.*, **88**, 598.
Green, R. F., and Morrill, M. E. 1978, *Pub. A.S.P.*, **90**, 601.
Green, R. F., and Schmidt, M. 1978, *Ap. J. (Letters)*, **220**, L1.
Greenstein, J. L. 1966, *Ap. J.*, **144**, 496.
———. 1977, *A.J.*, **81**, 323.
Huchra, J. P. 1976, Ph.D. thesis, California Institute of Technology.
Iben, I., Jr. 1965, *Ap. J.*, **142**, 1447.
———. 1966*a*, *Ap. J.*, **143**, 483.
———. 1966*b*, *Ap. J.*, **143**, 505.
———. 1966*c*, *Ap. J.*, **143**, 516.
———. 1967*a*, *Ap. J.*, **147**, 624.
———. 1967*b*, *Ap. J.*, **147**, 650.
———. 1968, *Ap. J.*, **154**, 581.
Lamb, D. Q., and Van Horn, H. M. 1975, *Ap. J.*, **200**, 306.
Luyten, W. J. 1958, *On the Frequency of White Dwarfs in Space* (Minneapolis: University of Minnesota Observatory).
———. 1963–1966, *Pub. Astr. Obs. Univ. Minnesota*, Vol. **3**, Nos. 13–18.
———. 1965, *First Conference on Faint Blue Stars* (Minneapolis: University of Minnesota Observatory).
Matsushima, S. 1969, *Ap. J.*, **158**, 1137.
McCook, G. P., and Sion, E. M. 1977, *Villanova Univ. Obs. Contr.*, Vol. **2** (Philadelphia: Villanova Press).
McCuskey, S. W. 1966, *Vistas in Astronomy*, **7**, 141.
Mestel, L. 1952, *M.N.R.A.S.*, **112**, 583.
Mestel, L., and Ruderman, M. A. 1967, *M.N.R.A.S.*, **136**, 27.
Oort, J. H. 1958, *Ric. Astr. Specola Vaticana*, **5**, 415.

Oort, J. H. 1965, in *Stars and Stellar Systems*, Vol. **5** (Chicago: University of Chicago Press), p. 455.
Ostriker, J. P., Richstone, D. O., and Thuan, T. X. 1974, *Ap. J. (Letters)*, **188**, L87.
Sandage, A., and Luyten, W. J. 1967, *Ap. J.*, **148**, 767.
———. 1969, *Ap. J.*, **155**, 913.
Schmidt, M. 1959, *Ap. J.*, **129**, 243.
———. 1963, *Ap. J.*, **137**, 758.
———. 1968, *Ap. J.*, **151**, 393.
———. 1975, *Ap. J.*, **202**, 22.
Schmidt, M., and Ulfbeck, O. 1977, private communication.
Sion, E. M., and Liebert, J. 1977, *Ap. J.*, **213**, 468.
Sletteback, A., Wright, R. R., and Graham, J. A. 1968, *A.J.*, **73**, 152.
Spitzer, L., and Schwarzschild, M. 1953, *Ap. J.*, **118**, 106.
Tapia, S. 1977, preprint.
Upgren, A. R. 1963, *A.J.*, **68**, 475.
Van Horn, H. M. 1968, *Ap. J.*, **151**, 227.
van Rhijn, P. J. 1929, *Pub. Kapteyn Astr. Lab.*, Groningen, No. 43.
———. 1936, *Pub. Kapteyn Astr. Lab.*, Gröningen, No. 47.
Wehrse, R. 1975, *Astr. and Ap.*, **39**, 174.
Weidemann, V. 1967, *Zs. Ap.*, **67**, 286.
———. 1975, in *Problems in Stellar Atmospheres and Envelopes* (Berlin: Springer-Verlag), p. 173.
———. 1978, in *IAU Symposium No. 80, The HR Diagram*, ed. A. G. Davis Philip and D. S. Hayes (Dordrecht: Reidel), p. 136.
Wickramasinghe, D. T., and Strittmatter, P. A. 1972, *M.N.R.A.S.*, **160**, 421.

RICHARD F. GREEN: Steward Observatory, University of Arizona, Tucson, AZ 85721

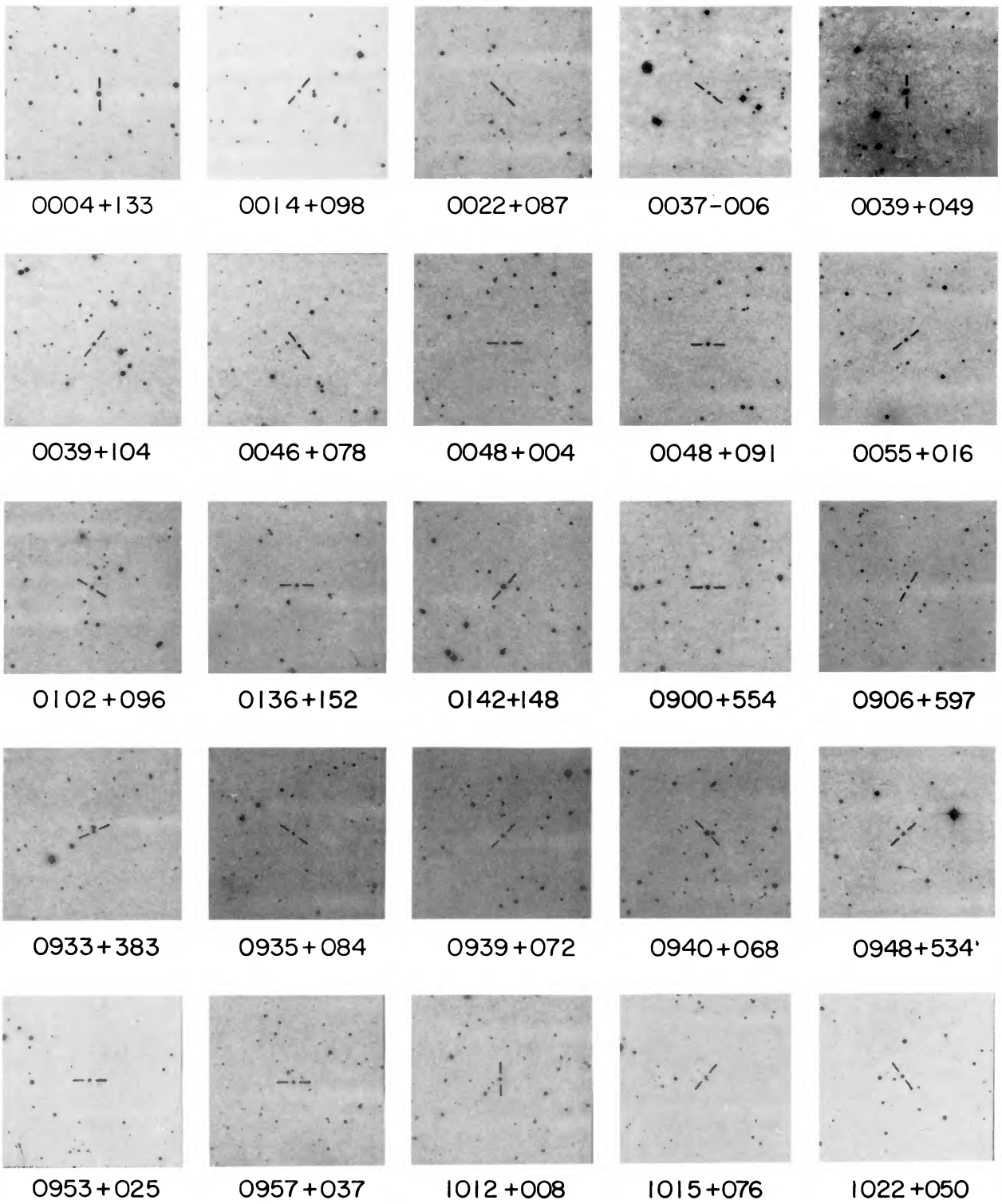

FIG. 4.—Finding charts for newly discovered probable white dwarfs (from Table 3). Each chart represents an area approximately 10′.5 on a side, with north at the top and east at the left. They are reproduced from the National Geographic–Palomar Sky Survey prints.

GREEN (*see* page 687)

PLATE 21

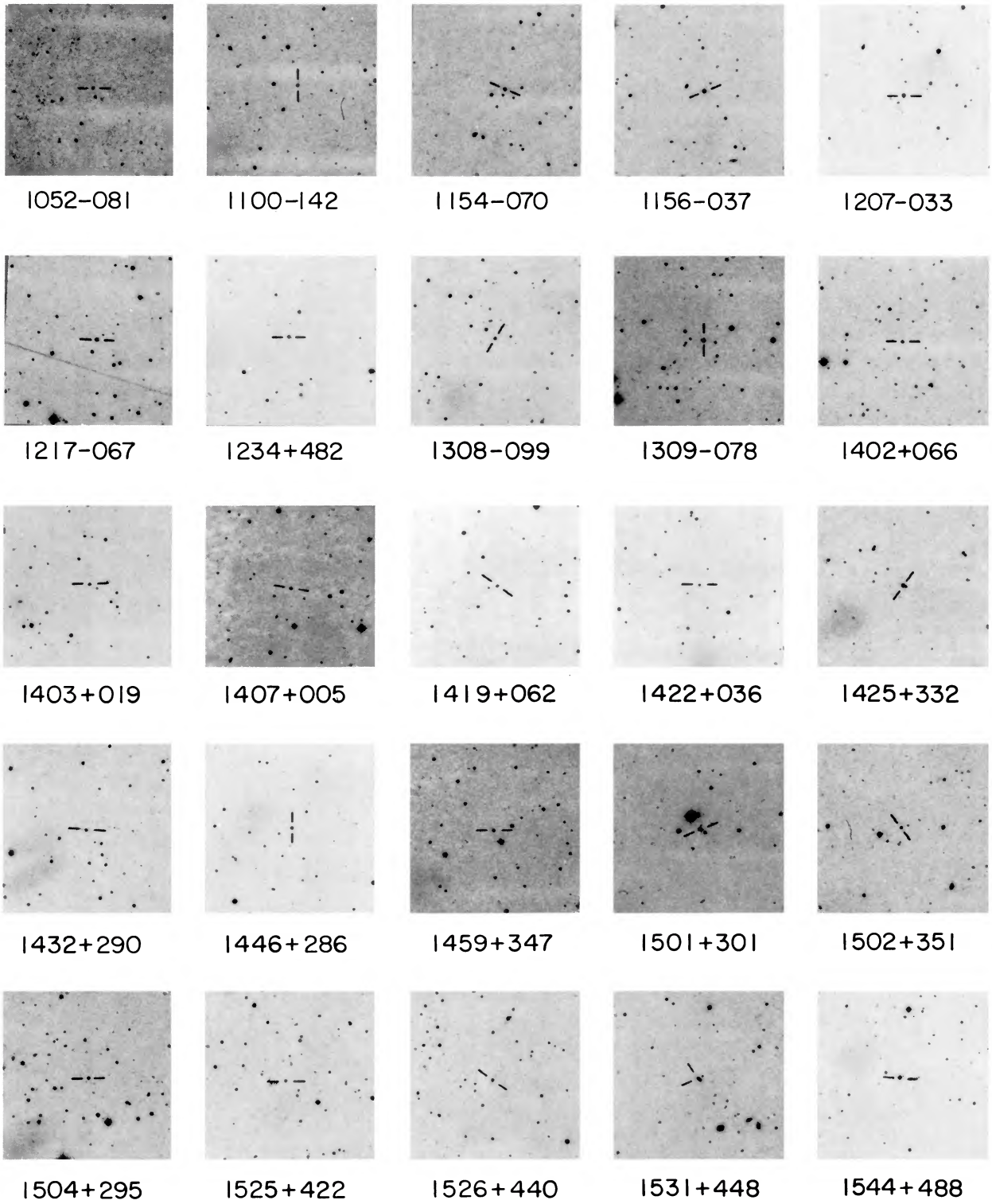

FIG. 4—*Continued*

GREEN (*see* page 687)

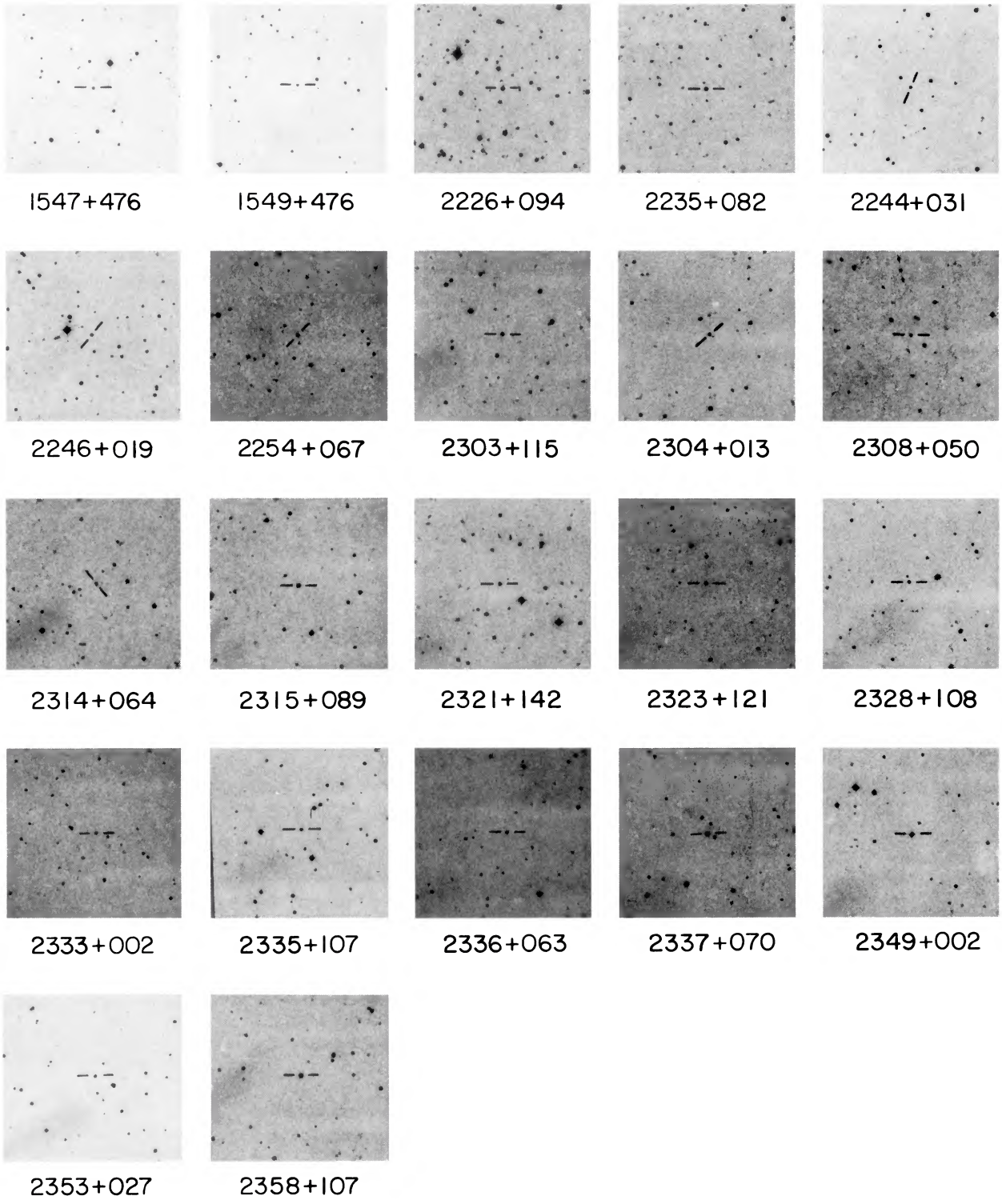

FIG. 4—*Continued*

GREEN (*see* page 687)